Volume 57
Number 22
18 March 2021
Pages 2699–2828

ChemComm

Chemical Communications

rsc.li/chemcomm

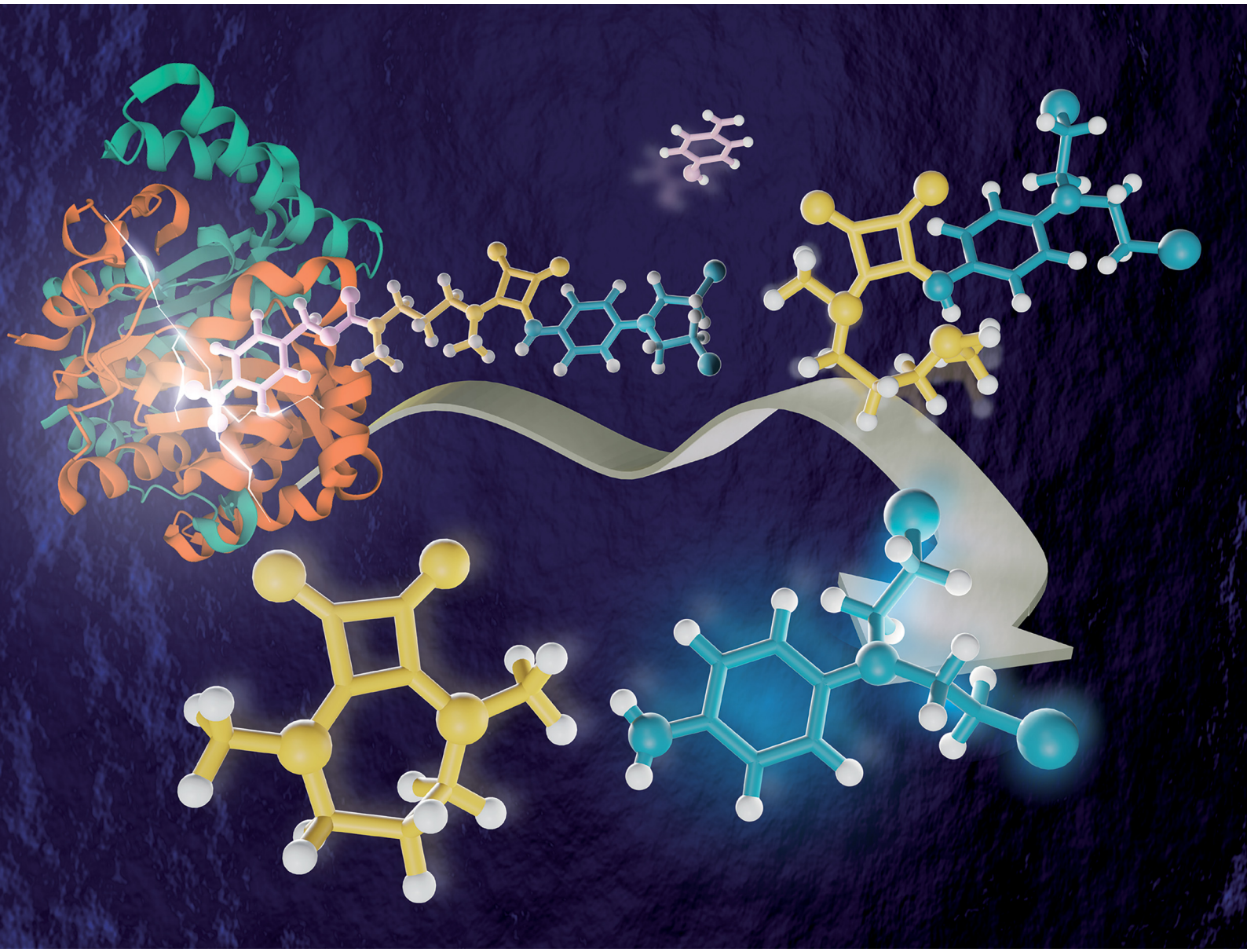

ISSN 1359-7345

ROYAL SOCIETY OF CHEMISTRY

COMMUNICATION

Carmen Rotger *et al.*

Introducing a squaramide-based self-immolative spacer for controlled drug release

ChemComm

COMMUNICATION

View Article Online
View Journal | View Issue

Cite this: *Chem. Commun.*, 2021, **57**, 2736

Received 23rd November 2020,
Accepted 9th February 2021

DOI: 10.1039/d0cc07683j

rsc.li/chemcomm

Introducing a squaramide-based self-immolative spacer for controlled drug release†

Marta Ximenis,[a] Angel Sampedro,[a] Luis Martínez-Crespo,[a] Guillem Ramis,[b] Francisca Orvay,[a] Antonio Costa[a] and Carmen Rotger[*a]

Herein we report the design, synthesis and assessment of the first example of a squaramide-based self-immolative system triggered by an enzymatic reduction. We have proved that the release of the alkylating agent *N*′,*N*′-(bis(2-chloroethyl)benzene)-1,4-diamine (ANM) provokes a dramatic reduction of the survival factor in glioblastoma cells, evidencing the suitability of the squaramide-based spacer for drug delivery applications.

Efficient drug delivery is a challenging issue owing to the poor pharmacokinetic properties of many bioactive compounds.[1] Prodrug design has become a successful strategy to upgrade their pharmacokinetic profile while voiding their pharmacological activity and unwanted side effects.[2,3] Ideally, prodrugs are enzymatically activated at their target within the organism, yielding the bioactive compound after the cleavage of labile bonds.[4,5] However, the steric requirements for a successful enzymatic cleavage step are sometimes difficult to fulfill.[6] The incorporation of self-immolative spacers within the prodrug structure increases the distance between the labile bond (trigger) and the drug moiety, favoring enzymatic cleavage.[7] In general, self-immolative spacers spontaneously undergo a cascade of disassembly reactions in response to an external stimulus, enabling a temporally sequential release of drug molecules.[8] These stimuli-responsive molecules disassemble through two main mechanisms: elimination and cyclization processes.[7] Many self-immolative spacers have been employed to construct drug delivery systems, but also sensors,[9,10] molecular amplifiers,[11–13] and stimuli-responsive materials.[14] Nevertheless, some self-immolative spacers have complex structures, which can be an issue for their large scale synthesis and commercial use. Therefore, there is a demand for, new self-immolative spacers of affordable synthesis and straightforward conjugation to drugs.[1] In this regard squaramides are remarkable compounds since they are easy to synthesize, capable of interacting with other molecules and have been successfully used as linkers in bioconjugate active compounds.[15]

Besides, squaramides are kinetically stable for periods longer than 100 days in the pH range of 3–10 at 37 °C.[16,17] Alkyl squaramates are also known for their remarkable stability in water, resisting hydrolysis at pH 7–9 for periods comprising several hours to days depending on the structure.[18]

Herein, we introduce the first example of a minimalist self-immolative spacer based on the squaramide moiety (**SQ-SIS**) that disassembles through a cyclization reaction with the simultaneous release of a leaving group (Fig. 1). Our design was inspired in our previous studies regarding the conformational properties of squaramides,[19,20] where we demonstrated that *N*-methyl squaramides favour the *E*,*Z* conformation either in the solid-state or in solution.[21] Thus, we hypothesised that preorganization offered by this conformation would promote the intramolecular attack of a nucleophile (trigger) located at

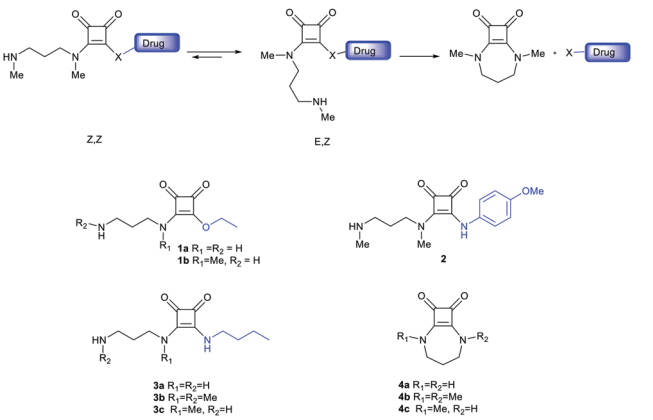

Fig. 1 Schematic showing the rational design of the squaramide-based self-immolative spacer **SQ-SIS** that disassembles through a cyclization reaction. Chemical structures of the ethyl squaramates **1a** and **1b**, squaramides **2** and **3a-3c**, and the cyclic squaramides **4a-4c**.

[a] *Universitat de les Illes Balears, Cra. Valldemossa Km 7.5, Palma de Mallorca 07122, Spain. E-mail: carmen.rotger@uib.es*

[b] *Institut Universitari d'Investigació en Ciències de la Salut (IUNICS), Universitat de les Illes Balears, and Institut d'Investigació Sanitària Illes Balears (IdISBa), Cra. Valldemossa Km 7.5, Palma, Illes Balears, Spain*

† Electronic supplementary information (ESI) available: Experimental details and analytical data for all new compounds. See DOI: 10.1039/d0cc07683j

the γ-position of one alkyl squaramide substituent enhancing the disassembly process. We designed **SQ-SIS** to form a seven-membered ring cyclic squaramide after the fragmentation reaction. The cyclization step yield drops for the corresponding six-membered analogues due to their inability to compensate for the cyclobutenedione ring strain, opening up the C=C–N bond angles and adopting a non-planar conformation.[22] The low cyclization efficiency is more significant when in water (pH ≥7) the ester group hydrolysis competes with the cyclization (see the ESI,† and S18).[18] Therefore, the kinetic control on the self-immolative reaction will be gained by the trigger activation through an external stimulus and by tuning the fugacity of the leaving group (Fig. 1).

In our design, we decorated the **SQ-SIS** with a primary or secondary alkyl amine group as a trigger since these groups are conveniently capped with a protecting group until receiving the corresponding stimulus. First, we evaluated the kinetic properties of the **SQ-SIS** by releasing different molecules of distinct nucleofugacity as drug models. For this purpose, we synthesized by sequential condensation of diethyl squarate with the corresponding amines, the ethyl squaramates **1a** and **1b**, and the squaramides **2** and **3b** (see the ESI,† Schemes S1 and S2) bearing ethanol, *n*-butylamine, and *p*-anisidine as leaving groups (Fig. 1) (see the ESI,† for synthetic details and compound characterization).

The self-immolative behaviour of the ethyl squaramate **1a** was evaluated at the pH range of 4.7–9 and 37 °C. The broad band in the UV spectrum of **1a** with a maximum at 275 nm was used to follow the reaction progress, observing its disappearance and the correlated appearance of a new band at 293 nm corresponding to the cyclization product **4a** (Fig. 2a).

The kinetic data were fitted to a pseudo-first-order rate law using ReactLabTM Kinetics to obtain the corresponding kinetic constants.[23] The cyclization reaction is pH sensitive in all the studied intervals and gets faster when increasing the pH.

The conversion of the ethyl squaramate **1a** into the cyclic squaramide **4a** is rapid even under moderate acidic conditions (pH 5, $k_{obs} = 0.65 \pm 0.01 \times 10^{-5}$ s^{-1}). At pH 7, the reaction gets 5.6 times faster (k_{obs} of $3.68 \pm 0.05 \times 10^{-5}$ s^{-1}), and at pH > 8, the conversion was too fast to be measured, observing only the band from product **4a**. The cyclization reaction gets faster for the *N*-Methylated analogue **1b** and even at pH 7 could not be measured, showing the effect of promoting the *E*,*Z* conformation on the reaction rate (see the ESI,† Fig. S18).

The formation of the cyclic squaramide **4a** was confirmed by ^{1}H-NMR (buffered D_2O-PBS at pH 7, 24 °C), following the appearance of a triplet at 3.7 ppm and a multiplet at 2.3 ppm corresponding to the α-and β-CH_2 of the cyclic compound, respectively, as well as the disappearance of the ethyl signals at 4.8 and 1.6 ppm (see the ESI,† Fig. S19–S21).[24] Similarly, squaramides **2** and **3b** were also evaluated by UV and ^{1}H-NMR spectroscopy, respectively (see the ESI,†Fig. 2b and c). Incubation of **2** in buffered solutions from pH 3–9 at 37 °C led again to a pH-dependent kinetic curve. The $k_{obs} = 5.74 \pm 0.1 \times 10^{-5}$ s^{-1} obtained for the cyclization reaction of the squaramide **2** at pH 7.4 resulted in the same order of magnitude as the k_{obs} obtained for the diethyl squaramate **1a**. However, the fitting of the ^{1}H-NMR data obtained from compound **3b** at pH 8 gave a $k_{obs} = 1.44 \times 10^{-5}$ s^{-1}, showing that the self-immolative reaction is, in this case, remarkably slower than for compounds **1a** and **2** (see the ESI,† Fig. S22 and S23). Thus, the temporary evolution of the three compounds at pH 7 and 37 °C depends on the nature of the leaving group and correlates well with the pK_a value of each group. After 8 h, the extent of the disassembly is insignificant (<1%) for compound **3b**, but much higher for compounds **2** (76%) and **1a** (97%), showing these two have a good profile for biological applications (Fig. 2d).

The positive effect of the squaramide *N*-methyl group on the cyclization step promoting the squaramide *E*,*Z* became again evident when we compared the kinetic constants obtained by ^{1}H-NMR (pH 8, 37 °C) of squaramides **3a** ($k_{obs} = 0.02 \times 10^{-5}$ s^{-1}) and **3c** ($k_{obs} = 0.07 \times 10^{-5}$ s^{-1}) showing a threefold increment in the cyclization rate for the *N*-methylated squaramide. Additionally, the trigger nucleophilicity also influences the overall cyclization reaction. Thus, **3b** ($k_{obs} = 1.44 \times 10^{-5}$ s^{-1}) having a secondary amine as a nucleophile disassembles roughly 20 fold faster than squaramide **3c** bearing a primary amine (see the ESI,† Fig. S23).

To gain control over the trigger activation, we used *p*-nitrobenzylcarbamate (*p*-NBzC), an enzymatically removable protecting group, to cap the trigger. The *p*-NBzC group is easily reduced by nitroreductases (NTR) in the presence of NADH as a reducing agent.[25] This protecting group, for which no associated toxicity has been reported, has been successfully applied in combined prodrug therapies.[10,26,27] Therefore, we synthesized squaramide **5a** and studied its enzyme triggered self-immolative reaction exposing the squaramide at pH 7.4 and 37 °C to the NTR/NADH tandem (5 μg mL^{-1} of NTR and 35 μM NADH), and monitored the self-immolative reaction by HPLC for 48 h. The enzymatic reduction and *p*-NBzC removal were

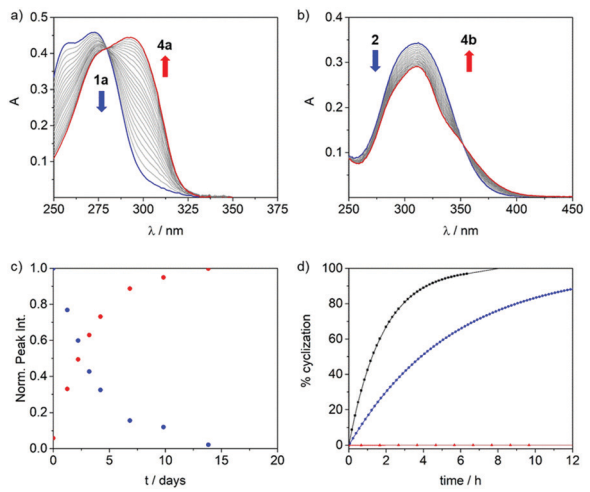

Fig. 2 Representative UV changes observed for the cyclization of (a) **1a** (PBS pH 5.7, 37 °C) and (b) **2** (PBS, pH 9 at 37 °C) (blue) to give **4a** and **4b**, respectively (red). (c) Disappearance of **3b** (blue) and appearance of **4b** (red) followed by ^{1}H-NMR (PBS pH 8–10 DMSO-d_6, 37 °C). (d) Percentage of cyclized squaramides **4a-4b** over time, comparing compounds **1a** (black), **2** (blue) and **3c** (red) at pH 7 and 37 °C.

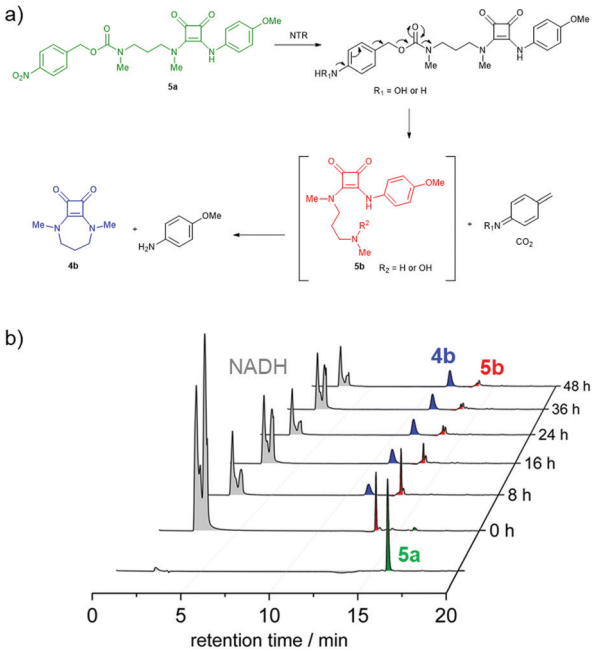

Fig. 3 (a) **5a** releases *p*-anisidine in response to the NTR/NADH tandem. (b) Time course plot of the disassembly reaction. The *p*-anisidine release rate was measured by the formation of cyclic squaramide **4b** (blue) using an HPLC-PDA detector set at 293 nm.

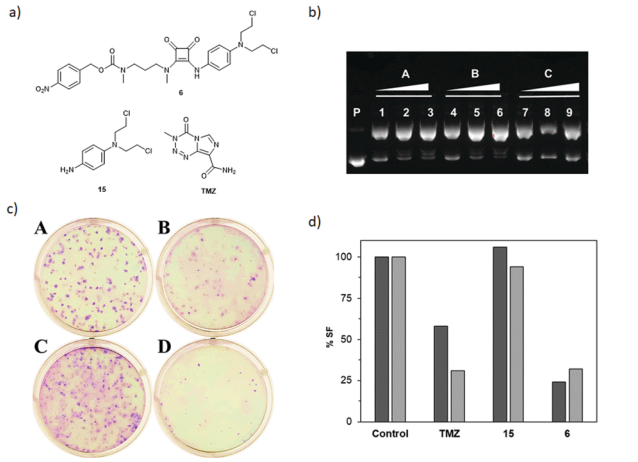

Fig. 4 (a) Chemical structure of compounds **6**, **15**, and temozolomide (TMZ). (b) DNA alkylation activity of **15** (A) and 6 (B and C) against plasmid p*max*-GFP by agarose gel electrophoresis. DNA was incubated for 48 h at pH 7.4 and 37 °C. Lane P, DNA control; lanes 1–3, 25, 50, and 100 μM of **15**; lanes 4–6, 25, 50, and 100 μM of **6** with the reduction tandem NRT/NADH; lanes 7–9, 25, 50, and 100 μM of **6** alone. (c) Representative clonogenic plates of U87-MG glioblastoma cells after 10 days comparing untreated cells (A) with cells treated with 10 μM of temozolomide (B), **15** (C), and **6** (D) for 1 h. (d) Representation of the Survival Factor index for LN229 (black) and U87-MG (grey) cells obtained from the clonogenic assay.

almost instantaneous to give squaramide **5b**. The intramolecular cyclization of **5b** went on within hours to yield the cyclic squaramide **4b** (Fig. 3b).‡

Once we had optimized the different elements of the self-immolative prodrug system, we synthesized compound **6** to evaluate the behaviour of the **SQ-SIS** by releasing a bioactive compound. Based on the previous experiments, we selected *N*′,*N*′-(bis(2-chloroethyl)benzene)-1,4-diamine **15** as a drug, which is a representative member of the Aniline Nitrogen Mustard (ANM) family (Scheme 1). The development of mustard-based hybrids is a known strategy for the discovery of anticancer drugs.[28,29] Squaramide **6** was obtained in two synthetic steps (see the ESI†). First, diethyl was subsequently condensed with the *p*-NBzC protected N^1,N^3-dimethylpropane-1,3-diamine, and then with **15** (see the ESI,† Schemes S3 and S4).

To determine the reactivity of compound **6** towards DNA, we performed a crosslinking assay using the Drew–Dickerson Dodecamer (**DDD**), a prototypical B-DNA.[30] Squaramide **6** (40 μM, 37 °C, pH, 7.4) and NTR/NADH (5 μg mL^{-1} and 35 μM respectively) were incubated with **DDD** (10 μM).

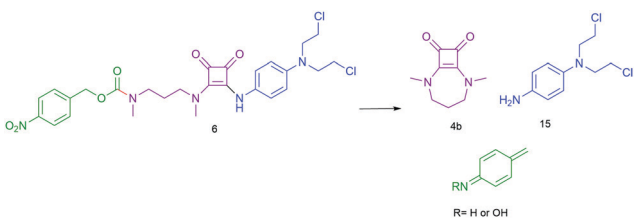

Scheme 1 Self-immolative disassembly of compound **6** triggered by enzymatic reduction of the nitro group.

The crude reaction mixture was analysed by ESI-HRMS (−) mode. The analysis of the mass spectra showed the mass peak corresponding to the single strand monoalkylated **DDD-15** adduct [3813.5982 (z = 1)], and peaks of multi charged species of the same adduct [1271.1994 (z = 3) and 953.3995 (z = 4)]. Additionally, the monoisotopic mass of the cyclic squaramide **4b** [181.0972 (z = 1)] was detected in ESI (+) mode (see the ESI,† and Fig. S27). The formation of the same **DDD-15** adduct and its multicharged species were detected when the free drug **15** was incubated with **DDD** (see Fig. S25, ESI†). DNA alkylation was also detected when compound **6** was incubated without the reduction tandem (see Fig. S26, ESI†). However in this case, along with the corresponding adduct **DDD-6** [4180.8627 (z = 1)], unreacted **DDD** and **6** were also detected. Therefore, we have detected the effective enzymatic release of compound **15** through the self-immolative cyclization step.

The DNA alkylation was also observed running a gel retardation assay after the incubation of compound **6** with the plasmid p*max*-GFP (3.4 kb) as a DNA source (Fig. 4).§ The plasmid was incubated for 48 h at pH 7.4 and 37 °C with increasing concentrations of **6** (0.25–1 × 10^{-4} M) and the reduction tandem NRT/NADH. The plasmid was incubated under the same conditions alone and with increasing concentrations of the free **15** (0.25 to 1 × 10^{-4} M) and **6** as control experiments. The agarose gel electrophoresis run from the reaction mixtures showed evident retardation on the DNA mobility in all the samples because of the plasmid alkylation. Similar DNA alkylation ratios were obtained in samples containing compounds **15** (lanes 1–3) and **6** with the reduction tandem (lanes 4–6). When incubated alone, compound **6** does not alkylate the plasmid to the same extent, which suggests that the activity of the drug is

reduced by the conjugation with the squaramide ring. This experiment also shows that the active free drug **15** has been efficiently released in samples containing the NTR/NADH enzymatic system.

Finally, we tested the self-immolative system **6** against two glioblastoma cultured cell lines (LN229 and U87-MG) by running a clonogenic assay, an *in vitro* cell survival assay based on the ability of a single cell to grow into a colony, to reveal the long-term DNA damage provoked by the alkylating agent. LN229 and U87-MG glioblastoma cells were treated with **6** for 1 h and then removed from the culture medium. The cells plated at low confluence concentrations (200 o 500 cells per well) were allowed to grow for 9 days. After this period, the colonies formed were stained and counted. The same procedure was applied to cells treated with temozolomide, a well-known alkylating agent widely used for the treatment of glioblastoma multi-form, the ANM **15**, and to untreated cells for comparison purposes.[31] The survival factor (SF) obtained for cells treated with **6** was 24% and 32% for LN229 and U87-MG cells respectively. These values are comparable with the SF obtained with temozolomide for U87-MG cells (31%) but sensibly lower than the SF observed for the LN229 cells (58%). Noteworthily cells treated with the free drug showed SF nearly of 100% in both lines, suggesting that our self-immolative prodrug has a positive effect on the drug stabilization and cell internalization, enhancing its activity after the intracellular activation of **6** by endogenous reductases.[32]

In conclusion, we have reported the first example of a squaramide-based self-immolative module **SQ-SIS** with suitable properties for drug release applications. **SQ-SIS** resists hydrolysis in physiological conditions and, after receiving an external stimulus, evolves through a cyclization reaction releasing different types of leaving groups. Still, aromatic amines are the most suitable compounds to conjugate with the module due to its moderate release rate at a useful pH interval for biological applications. Conjugation of **SQ-SIS** with *p*-nitrobenzylcarbamate, and the aromatic nitrogen mustard **15**, yields the enzymatic triggered self-immolative prodrug **6**. Under enzymatic reduction conditions, **6** disassembles, releasing the alkylating agent **15**. *In vitro* experiments and the clonogenic assays with U87-MG and LN229 glioblastoma cells proved the drug activity and the subsequent DNA damage. The low survival factor observed for cells treated with **6** suggests that the squaramide-based delivery system positively effects the drug activity.

We gratefully acknowledge the financial support from MINECO (projects CTQ2017-85821-R, AEI/FEDER, UE funds, CTQ2017-90852-REDC red, RED2018-102331-T), M. X. thanks Govern de les Illes Balears for a predoctoral fellowship, FSE funds.

Conflicts of interest

There are no conflicts to declare.

Notes and references

‡ No toxicity was found for concentrations of **4b** up to 200 μM.
§ Plasmid pmax-GFP encodes the green fluorescent protein.

1 A. G. Cheetham, R. W. Chakroun, W. Ma and H. Cui, *Chem. Soc. Rev.*, 2017, **46**, 6638–6663.
2 V. J. Stella, *J. Pharm. Sci.*, 2010, **99**, 4755–4765.
3 A. Najjar, A. Najjar and R. Karaman, *Molecules*, 2020, **25**, 284.
4 R. Walther, J. Rautio and A. N. Zelikin, *Adv. Drug Delivery Rev.*, 2017, **118**, 65–77.
5 J. Rautio, H. Kumpulainen, T. Heimbach, R. Oliyai, D. Oh, T. Järvinen and J. Savolainen, *Nat. Rev. Drug Discovery*, 2008, **7**, 255–270.
6 (*a*) A. D. Wong, M. A. DeWit and E. R. Gillies, *Adv. Drug Delivery Rev.*, 2012, **64**, 1031–1045; (*b*) P. L. Carl, P. K. Chakravarty and J. A. Katzenellenbogen, *J. Med. Chem.*, 1981, **24**, 479–480.
7 A. Alouane, R. Labruère, T. L. Saux, F. Schmidt and L. Jullien, *Angew. Chem., Int. Ed.*, 2015, **54**, 7492–7509.
8 C. Zang, H. Wang, T. Li, Y. Zhang, J. Li, M. Shang, J. Du, Z. Xi and C. Zhou, *Chem. Sci.*, 2019, **10**, 8973–8980.
9 J. Yan, S. Lee, A. Zhang and J. Yoon, *Chem. Soc. Rev.*, 2018, **47**, 6900–6916.
10 S. Gnaim and D. Shabat, *Acc. Chem. Res.*, 2014, **47**, 2970–2984.
11 M. Avital-Shmilovici and D. Shabat, *Soft Matter*, 2010, **6**, 1073–1080.
12 Q. Mou, Y. Ma, X. Jin and X. Zhu, *Mol. Syst. Des. Eng.*, 2016, **1**, 25–39.
13 M. E. Roth, O. Green, S. Gnaim and D. Shabat, *Chem. Rev.*, 2016, **116**, 1309–1352.
14 L. A. Marchetti, K. L. Kumawat, N. Mao, J. C. Stephens and R. B. P. Elmes, *Chemistry*, 2019, **5**, 1398–1485.
15 (*a*) R. I. Storer, C. Aciro and L. H. Jones, *Chem. Soc. Rev.*, 2011, **40**, 2330–2346; (*b*) K. A. Agnew-Francis and C. M. Wiliams, *Chem. Rev.*, 2020, **120**, 11616–11650.
16 M. Ximenis, E. Bustelo, A. G. Algarra, M. Vega, C. Rotger, M. G. Basallote and A. Costa, *J. Org. Chem.*, 2017, **82**, 2160–2170.
17 K. H. Glüsenkamp, W. Drosdziok, G. Eberle, E. Jähde and M. R. Rajewsky, *Z. Naturforsch.*, 1991, **46c**, 498–501.
18 M. Ximenis, Doctoral dissertation, University of Balearic Islands, Palma, 2019.
19 L. Martínez, G. Martorell, A. Sampedro, P. Ballester, A. Costa and C. Rotger, *Org. Lett.*, 2015, **17**, 2980–2983.
20 M. C. Rotger, M. N. Piña, A. Frontera, G. Martorell, P. Ballester, P. M. Deyà and A. Costa, *J. Org. Chem.*, 2004, **69**, 2302–2308.
21 L. Martínez-Crespo, E. C. Escudero-Adán, A. Costa and A. C. Rotger, *Chem. – Eur. J.*, 2018, **24**, 17802–17813.
22 (*a*) W. A. Kinney, M. Abou-Gharbia, D. T. Garrison, J. Schmid, D. M. Kowal, D. R. Bramlett, T. L. Miller, R. P. Tase, M. M. Zaleska and J. A. Moyer, *J. Med. Chem.*, 1998, **41**, 236–246; (*b*) M. Ximenis, J. Pitartch-Jarque, S. Blasco, C. Rotger, E. García España and A. Costa, *Cryst. Growth Des.*, 2018, **18**, 4420–4427.
23 P. King and M. Maeder, *Multivariate Analytical Technologies*, Jplus Consulting, East Fremantle, Australia, 2009.
24 P. K. Glasoe and F. A. Long, *J. Phys. Chem.*, 1960, **64**, 188–190.
25 B. M. Sykes, M. P. Hay, D. Bohinc-Herceg, N. A. Helsby, C. J. O'Connor and W. A. Denny, *Perkin 1*, 2000, 1601–1608.
26 S. K. Sharma and K. D. Bagshawe, *Adv. Drug Delivery Rev.*, 2017, **118**, 2–7.
27 J. Zhang, V. Kale and M. Chen, *AAPS J.*, 2015, **17**, 102–110.
28 R. K. Singh, S. Kumar, D. N. Prasad and T. R. Bhardwaj, *Eur. J. Med. Chem.*, 2018, **151**, 401–433.
29 A. P. Mishra, S. Chandra, R. Tiwari, A. Srivastava and G. Tiwari, *Open Med. Chem. J.*, 2018, **12**, 111–123.
30 R. Wing, H. Drew, T. Takano, C. Broka, S. Tanaka, K. Itakura and R. E. Dickerson, *Nature*, 1980, **287**, 755–758.
31 J. Zhang, M. F. G. Stevens and T. D. Bradshaw, *Curr. Mol. Pharmacol.*, 2012, **5**, 102–114.
32 Y. Liu, W. Yan, H. Li, H. Peng, X. Suo, Z. Li, H. Liu, J. Zhang, S. Wang and D. Liu, *Anal. Methods*, 2019, **11**, 421–426.